

TLR7-expressing cells comprise an interfollicular epidermal stem cell population in
murine epidermis

Author list:

Chaoran Yin

Ting Zhang

Liangjun Qiao

Jia Du

Shuang Li

Hengguang Zhao

Fangfang Wang

Qiaorong Huang

Wentong Meng

Hongyan Zhu

Hong Bu

Hui Li

Hong Xu

Xianming Mo

Supplementary data

Fig. S1. Activation and suppression of TLR7 via imiquimod and IRS661 in vivo.

(A-G) View of the dorsal skin. Imiquimod treated mice (A); Imiquimod and IRS661 treated mice (B); Imiquimod and control ODN treated mice (C); DMSO treated mice (D); DMSO and IRS661 treated mice (E); DMSO and control ODN treated mice (F); Untreated mice (G). The flakes and rash in the regions demarcated by white dashed lines in (A-C). (H-K') IRS661-cy3 and control ODN-cy3 diffused in epidermis. Epidermal side view in (H-K'); Fluorescent field (H-K); Bright field (H'-K').

Fig. S2. Unstained activation of TLR7 mediated by imiquimod caused aberrant proliferation of interfollicular cells.

(A-F) Immunohistochemistry with the mitosis associated marker H3pS10 showed the proliferative epidermal cells. Black dashed lines outlined the epidermal region. Imiquimod treated skin (A); Imiquimod and IRS661 treated skin (B); Imiquimod and control ODN treated skin (C); DMSO treated skin (D); DMSO and IRS661 treated skin (E); DMSO and control ODN treated skin (F). (G) Quantification of the proliferation of epidermal interfollicular cells in A-F.

Fig. S3. Imiquimod treatment stimulated the proliferation of basal layer cells

(A-F) EdU-label cells were examined in imiquimod (A); Imiquimod combined with IRS661 treatment (B); Imiquimod combined with control ODN (C); DMSO (D); DMSO combined with IRS661 treatment (E) or DMSO combined with control ODN (F) treated skin. The dashed outlined the basal layer highlighted by ITGA6 staining. **: $P < 0.01$, t-test.

Fig. S4. Imiquimod treatment induced K17 ectopic expression.

(A, B) Immunofluorescence revealed K17 ectopic expression in the hyperplastic epidermis induced by imiquimod treatment. Arrowheads indicated the ectopic expression of K17. IFE, interfollicular epidermis. (C) RT-PCR detected the

expression level of krt17 between DMSO and imiquimod -treated skin. Quantification of the result of RT-PCR. * $P < 0.05$ versus control, t-test.

Fig. S5. FACS analysis of TLR7 expression in epidermal keratinocytes from mouse skin.

(A, B) Unicellular suspension of keratinocytes harvested from epidermis was stained for TLR7 and Lin and analyzed by FACS. Flow cytometric analysis of TLR7-labelled cells (A) versus isotype control (B) indicated that TLR7-positive cells represent about 2% of the Lin-negative cells. (C) TLR7 expressed on the membrane of FACS-sorted TLR7-positive keratinocytes.

Fig. S6. The TLR7-antibodies were able to detect the mouse TLR7 protein specifically. (A) Western blot was performed using sc-16245 and IMG-581A antibodies. (B, C) Immunofluorescent staining of mouse spleen and brain sections with sc-16245 antibody.

Fig. S7. TLR7 positive population comprised two subsets respectively display characteristics of epidermal stem cells and hair follicle stem cells. Analysis of the differentiation potential of different populations of epidermis by immunofluorescence. (A, B) The colonies derived from TLR7⁺/ITGA6⁺, TLR7⁺/ITGA6⁻, TLR7⁻/ITGA6⁺ and All (the unfractionated population) were immunofluorescently stained with antibodies against hair-specific (AE13), sebaceous gland (PPAR γ) and epidermal (K1) differentiation markers. Cells from triplicate experiments were counted. (C, D) The colonies derived from TLR7⁺/CD34⁺, TLR7⁺/CD34⁻, TLR7⁻/CD34⁺ and All (the unfractionated population) were immunofluorescently stained with antibodies against hair-specific (AE13), sebaceous gland (PPAR γ) and epidermal (K1) differentiation markers. Cells from triplicate experiments were counted.

Fig. S8. FACS plots for the assessment of TLR7-positive keratinocytes sorted by magnetic cell sorting.

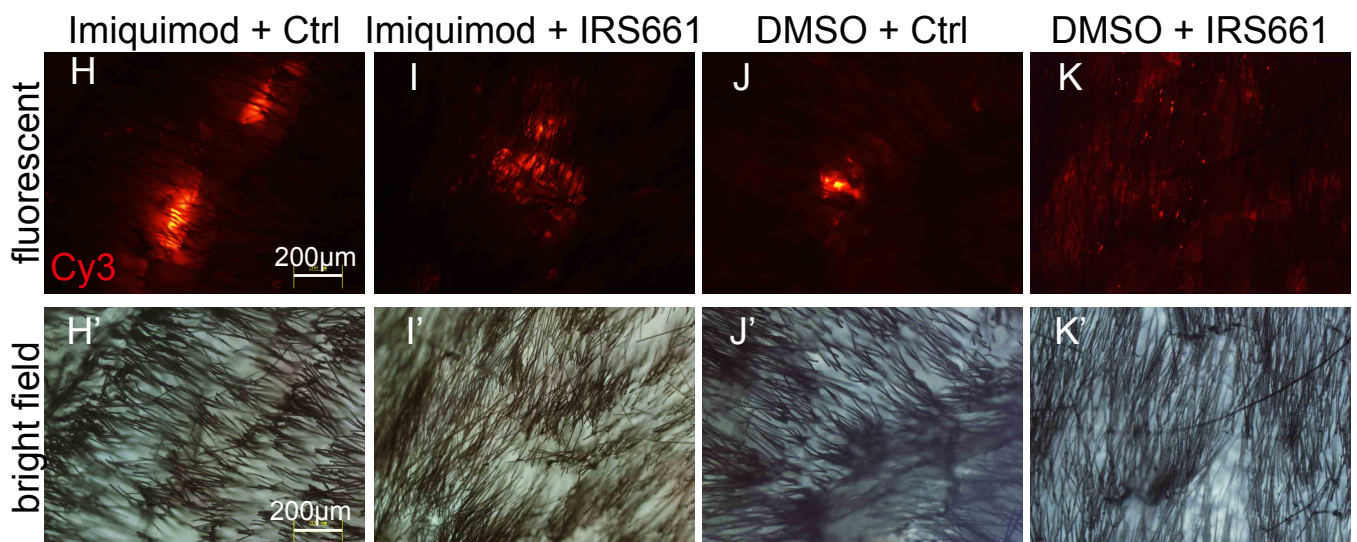
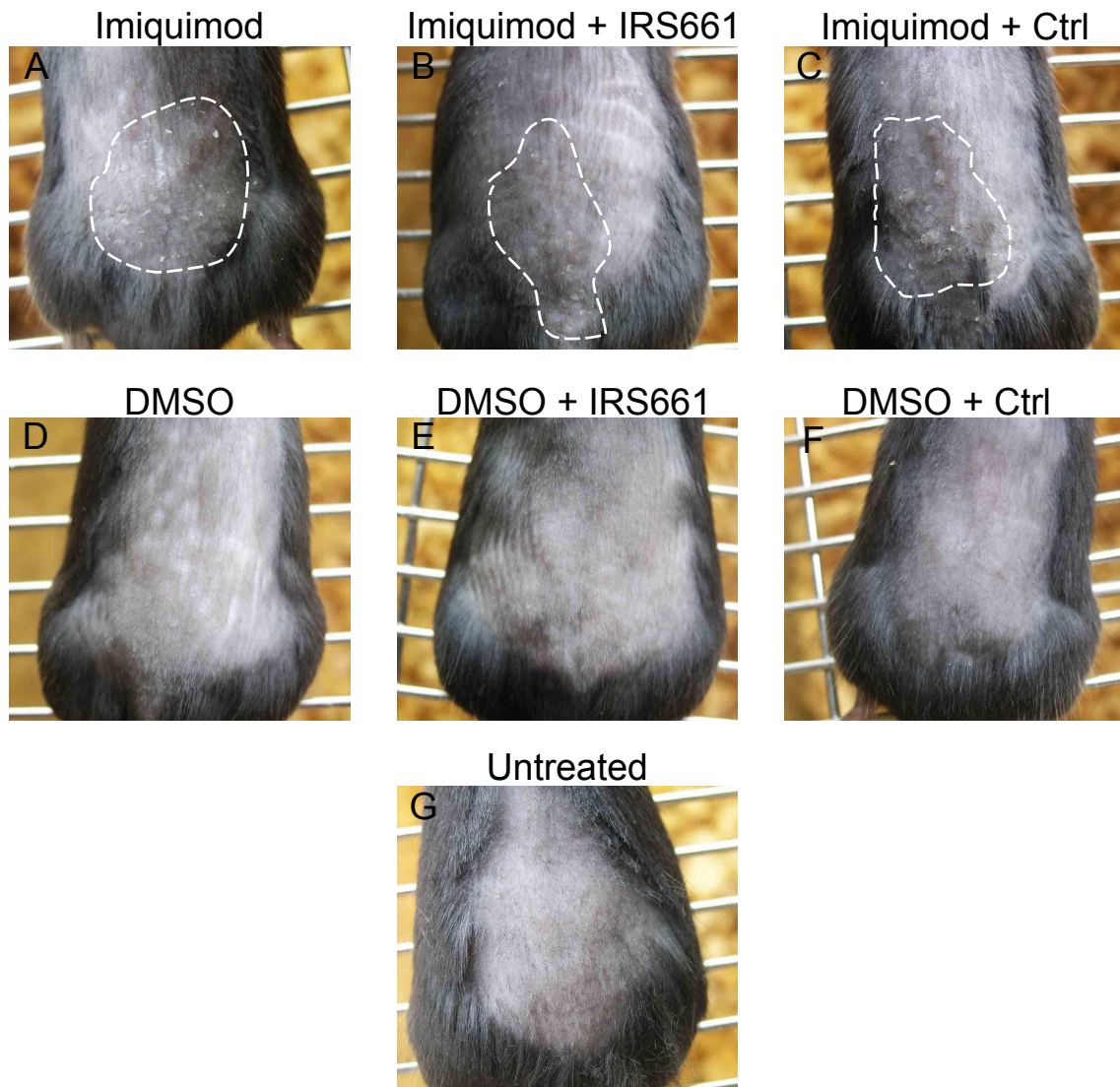
(A-B') Primary cells isolated from dorsal skin of mice were labeled with TLR7 antibody, biotinylated antibody and BDTM IMag streptavidin particles-DM. After labeling, the cells were separated using the BDTM IMagnet, and the positive (TLR7⁺) fraction was collected. For flow cytometric analysis, the positive fraction was stained with TLR7 antibody and AlexFluor 488 donkey anti-rabbit IgG. The percentage of positive cells is given in (A', B'); TLR7-labelled cells (A, A') versus isotype control (B, B'). All techniques were performed according to the manufacturer's guidelines.

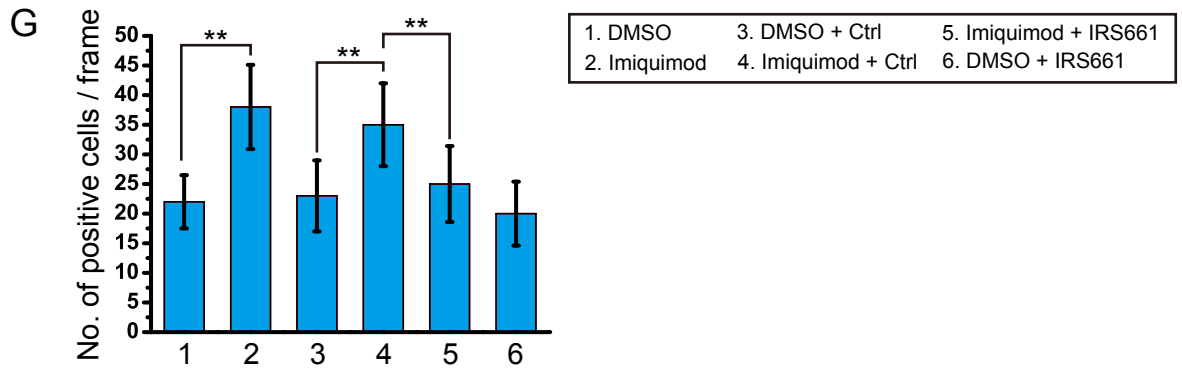
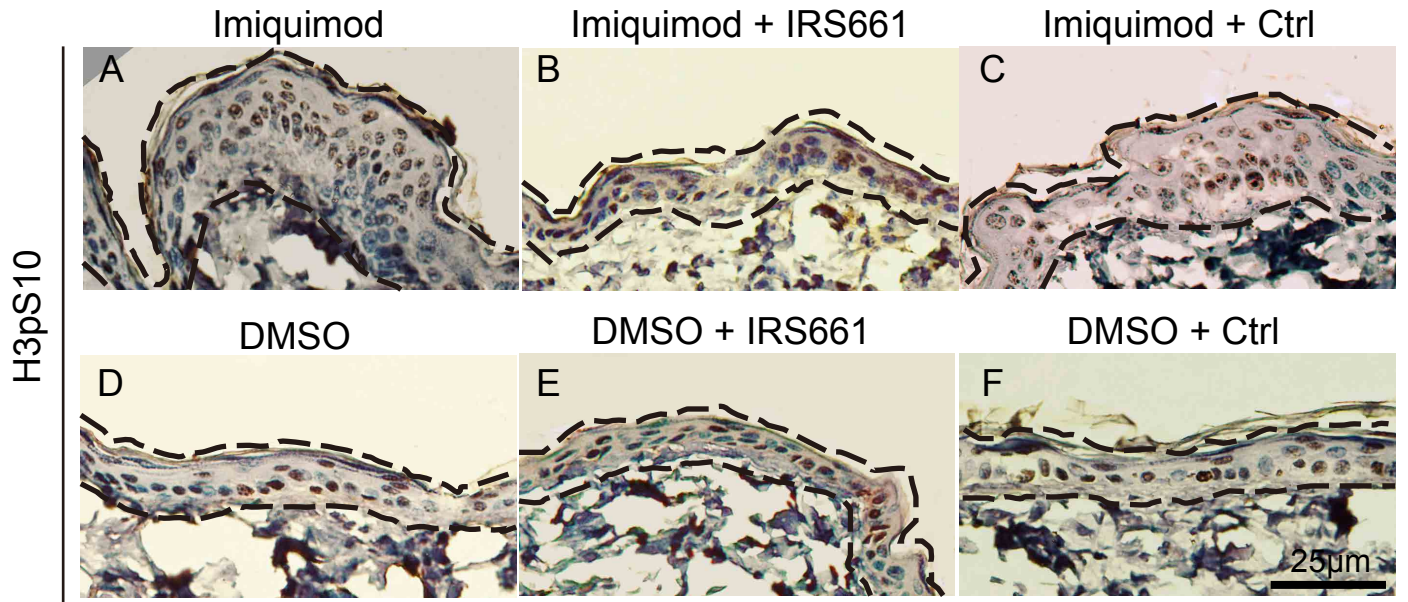
Fig. S9. Serial transplantation in vivo.

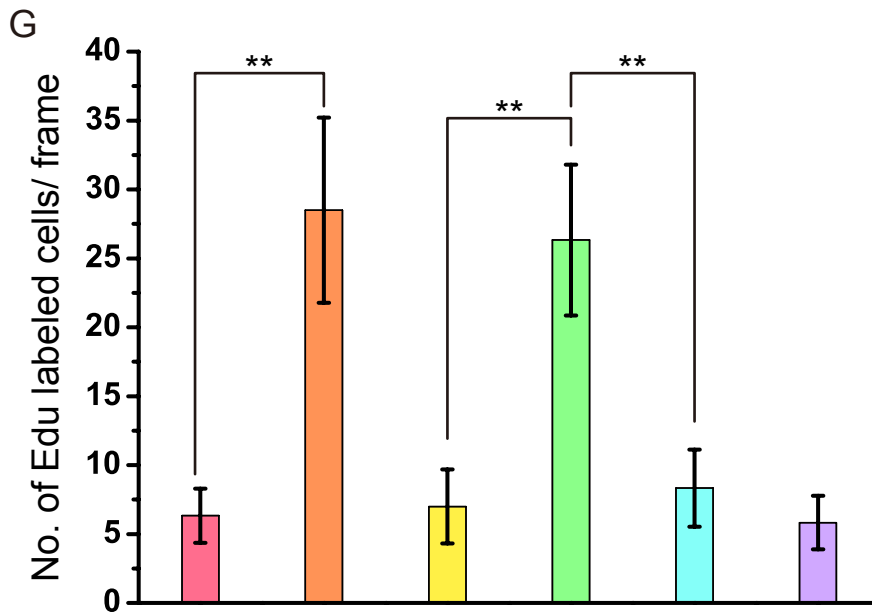
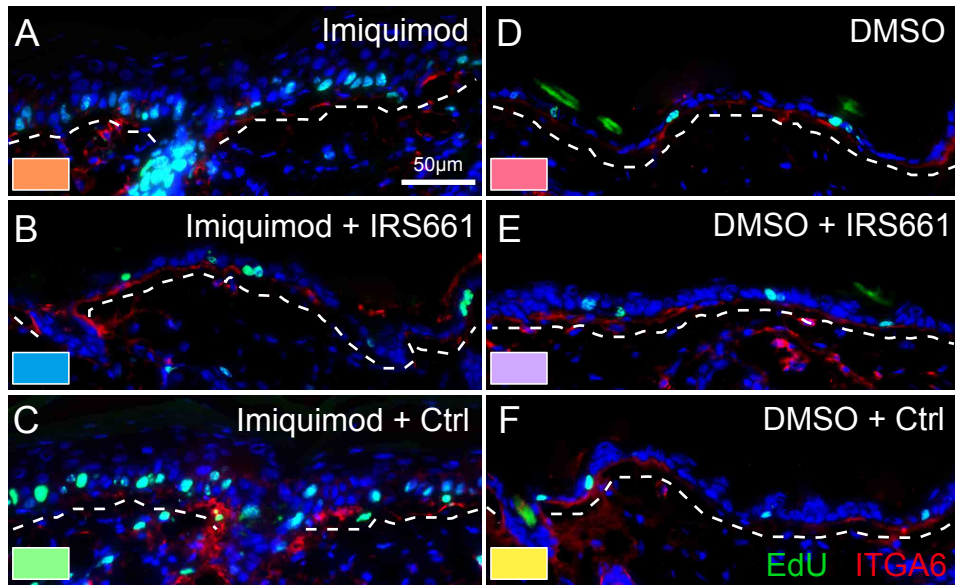
(A-C) Cells from EGFP mice mixed with dermal cells reconstitute fully formed or did not generate skin and hair. Images of grafts were photographed three weeks post-transplantation: the unfractionated population of epidermis mixed with dermal cells (All+dermal) (A), TLR7-positive cells with dermal cells (TLR7⁺+dermal) (B), and TLR7-negative cells with dermal cells (TLR7⁻+dermal) (C). (D, E) Epidermal view of the graft. (F, G) Epidermal view of graft. (F) EGFP-positive cells contributed to the skin. The white arrowhead indicates reconstructed epidermis revealing EGFP fluorescence. Region in (a) is a higher magnification of the region marked by the white dashed line in (F), and the white arrowhead shows the reconstituted hair. (G) Higher magnification shows the EGFP-positive epidermal cells in the second graft.

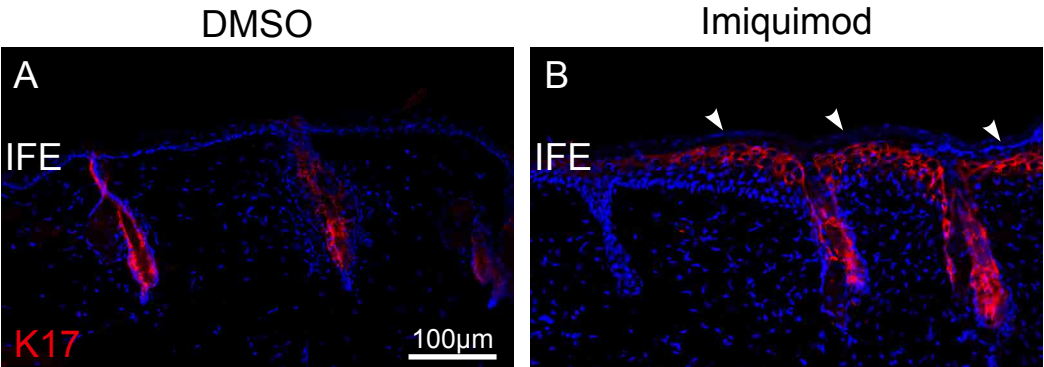
Fig. S10. The experimental approach for serial transplantation.

(A, C) Primary TLR7-expressing keratinocytes isolated or unsorted cells from dorsal skin of EGFP mice were subjected to full-thickness replacement grafting onto dorsal skin of a nude mouse, and then formed the primary graft. (B, D) These cells were implanted onto the back of another nude mouse, and then formed the second graft. (E) The primary graft was digested into cell suspension.

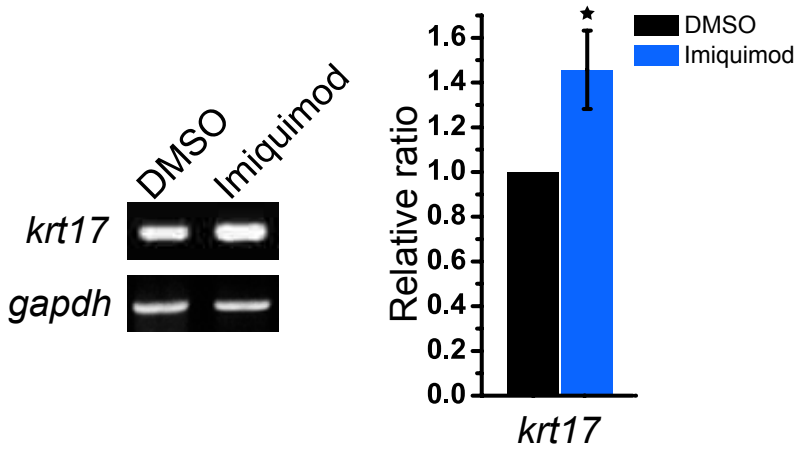


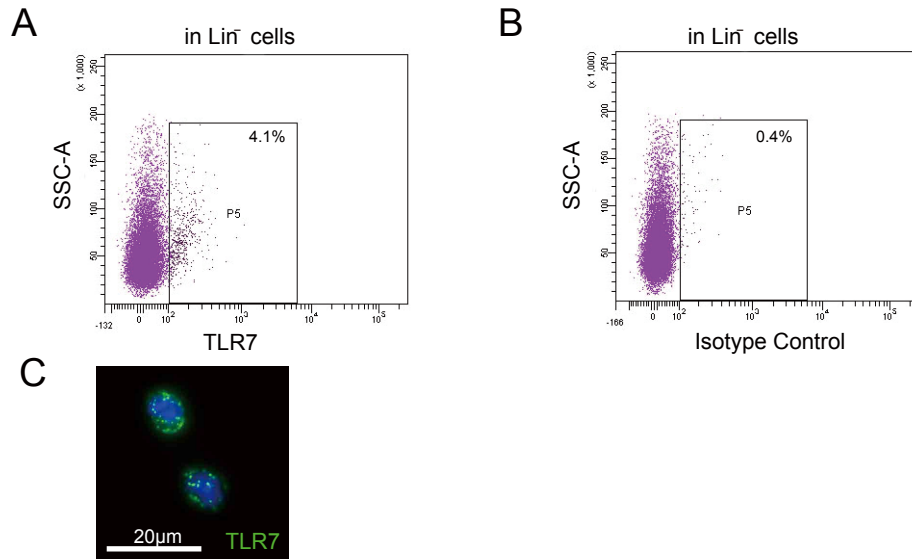


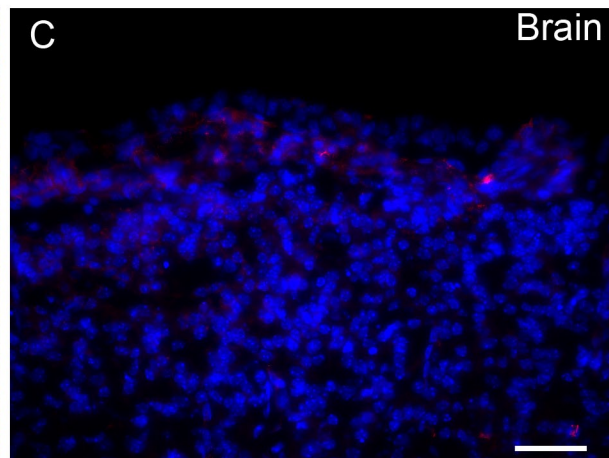
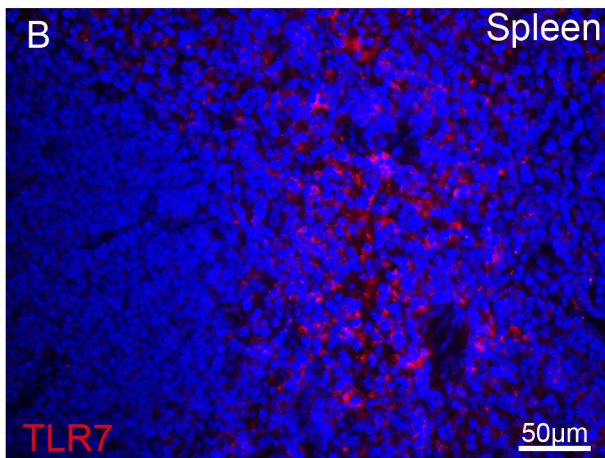
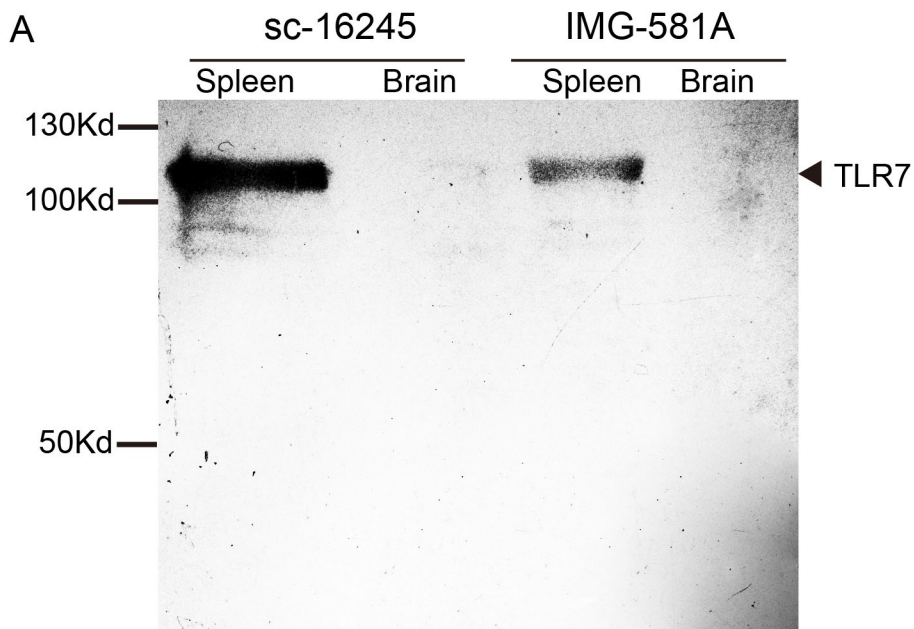


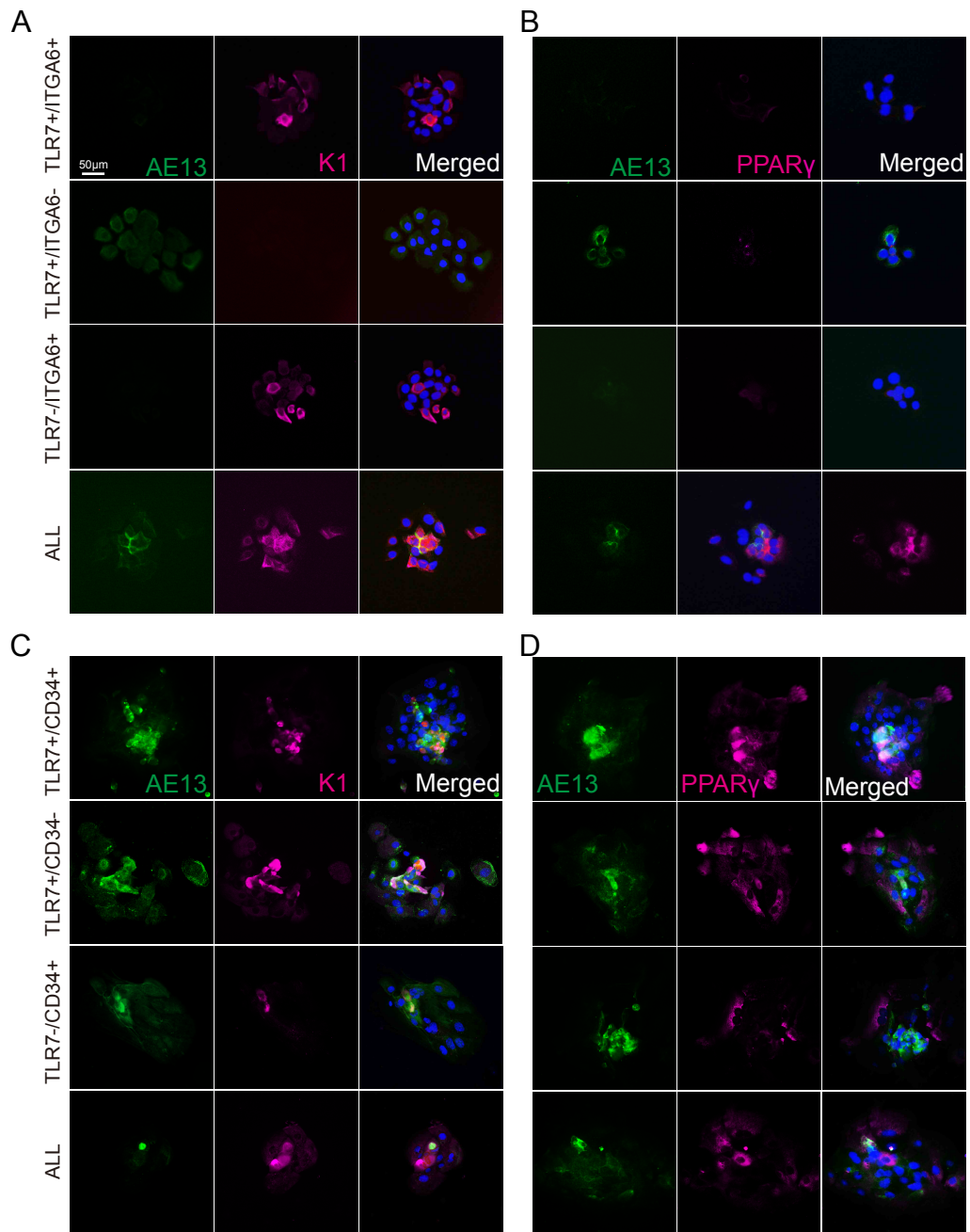


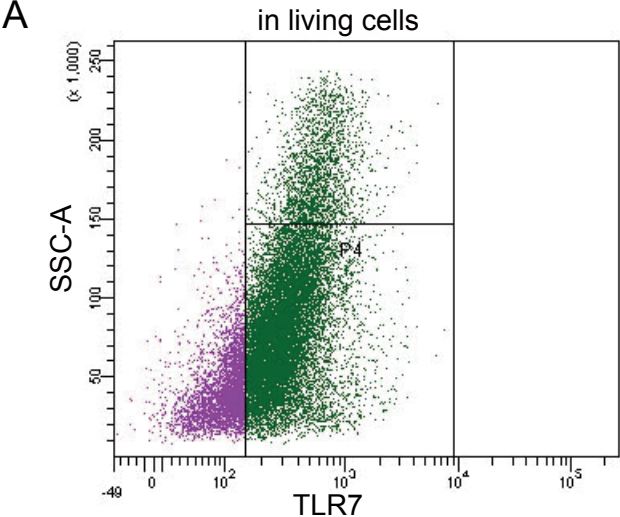
C





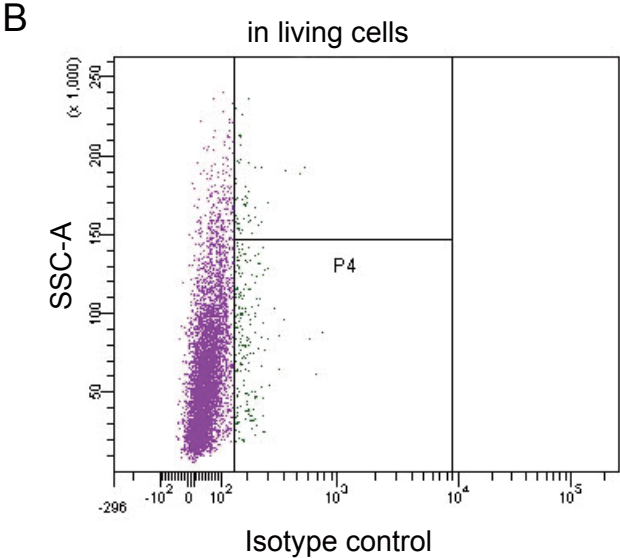






A'

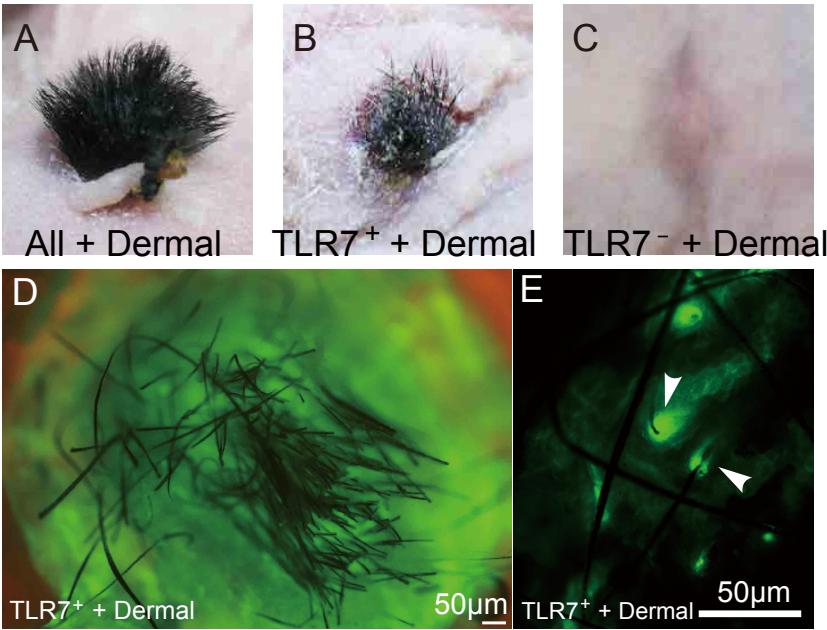
Population	#Events	%Parent	%Total
All Events	30,000		100.0
P1	23,259	77.5	77.5
P2	20,398	87.7	68.0
P3	20,291	99.5	67.6
P4	16,546	81.5	55.2



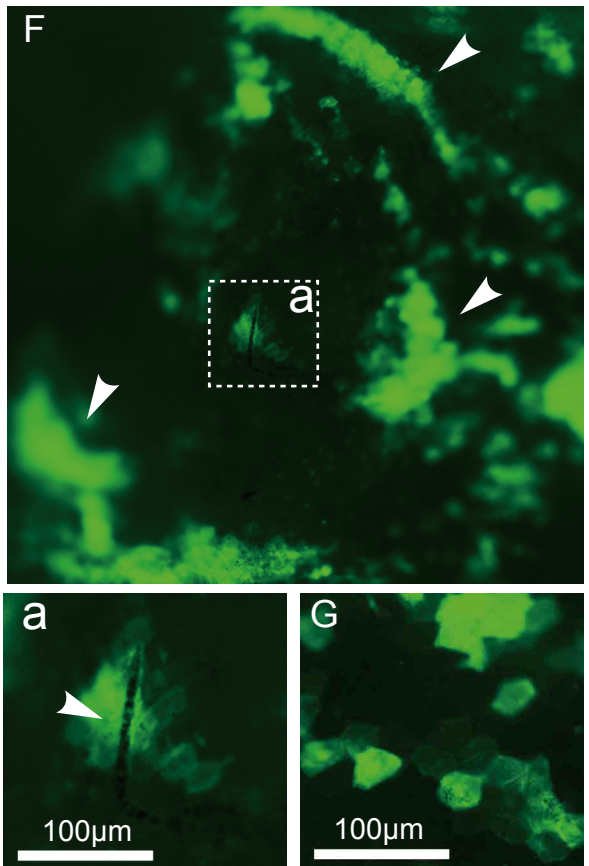
B'

Population	#Events	%Parent	%Total
All Events	9,594		100.0
P1	7,816	81.5	81.5
P2	5,773	73.9	60.2
P3	5,769	99.9	60.1
P4	236	4.1	2.5

First transplantation



Secondary transplantation



Supplementary Figure 10

First transplantation



Secondary transplantation



Dissociated cells

